Table I. Fractional Coordinates ($\times 10^4$) for Non-Hydrogen Atoms with Their Standard Deviations and Equivalent Temperature Factors

	x/a	*y/b*	*z/c*	B_{eq}, Å^2
Zn1	2534 (1)	3877 (1)	9733 (1)	4.24
Br1	4183 (1)	2691 (1)	9693 (1)	5.66
Br2	811 (1)	2717 (1)	9594 (1)	6.39
S1	3005 (2)	4038 (3)	11635 (1)	4.80
S2	2157 (2)	4849 (2)	8017 (1)	4.80
N1	2531 (4)	6106 (6)	9955 (4)	3.18
C1	2724 (5)	7027 (7)	9336 (5)	3.50
C2	2680 (5)	8512 (8)	9444 (5)	4.46
C3	2437 (6)	9061 (9)	10211 (6)	5.29
C4	2246 (6)	8113 (9)	10837 (6)	4.90
C5	2296 (5)	6648 (8)	10713 (5)	3.64
C6a	2064 (6)	5573 (9)	11381 (5)	4.67
C6b	3023 (6)	6363 (9)	8531 (5)	5.01
C7a	4358 (6)	4927 (10)	12126 (6)	5.71
C7b	774 (6)	5670 (9)	7659 (6)	5.94
C8a	4483 (7)	5766 (11)	13008 (7)	7.24
C8b	-75 (7)	4583 (13)	7085 (7)	8.08

Table II. Structural Parameters

a. Bond Lengths (Å) with Standard Deviations

Zn1-Br1	2.368 (1)	C1-N1	1.336 (8)
Zn1-Br2	2.375 (1)	C5-N1	1.358 (8)
S1-Zn1	2.741 (2)	C2-C1	1.383 (10)
S2-Zn1	2.632 (2)	C6b-C1	1.504 (10)
N1-Zn1	2.083 (5)	C3-C2	1.378 (11)
C6a-S1	1.812 (8)	C4-C3	1.359 (11)
C7a-S1	1.834 (8)	C5-C4	1.368 (10)
C6b-S2	1.796 (8)	C6a-C5	1.503 (10)
C7b-S2	1.826 (7)	C8a-C7a	1.501 (13)
		C8b-C7b	1.527 (12)

b. Bond Angles in (deg) with Standard Deviations

Br2-Zn1-Br1	125.3 (1)	C1-N1-Zn1	120.4 (4)
S1-Zn1-Br1	98.0 (1)	C5-N1-Zn1	120.6 (4)
S1-Zn1-Br2	90.9 (1)	C5-N1-C1	118.9 (6)
S2-Zn1-Br1	91.7 (1)	C2-C1-N1	121.8 (6)
S2-Zn1-Br2	100.5 (1)	C6b-C1-N1	116.5 (6)
S2-Zn1-S1	157.0 (1)	C6b-C1-C2	121.7 (7)
N1-Zn1-Br1	120.3 (1)	C3-C2-C1	119.2 (7)
N1-Zn1-Br2	114.3 (1)	C4-C3-C2	118.4 (7)
N1-Zn1-S1	77.9 (2)	C5-C4-C3	121.0 (7)
N1-Zn1-S2	79.2 (2)	C4-C5-N1	120.6 (7)
C6a-S1-Zn1	84.5 (2)	C6a-C5-N1	117.1 (6)
C7a-S1-Zn1	108.7 (3)	C6a-C5-C4	122.3 (6)
C7a-S1-C6a	101.8 (4)	C5-C6a-S1	114.1 (4)
C6b-S2-Zn1	86.6 (2)	C1-C6b-S2	113.1 (5)
C7b-S2-Zn1	107.4 (3)	C8a-C7a-S1	114.8 (6)
C7b-S2-C6b	101.8 (4)	C8b-C7b-S2	109.6 (6)

The common stoichiometry presented by all these complexes suggested, as we had initially thought, that compound IIa behaves as a tricoordinated ligand, via the nitrogen and the sulfur atoms.

More confusing are the ^{1}H NMR data of IIa and Zn(IIa)Br_2 with regard to the denticity of the ligand. Because of the sulfur coordination to the zinc ion, an NMR shift of the sulfur-bonded methylene protons $CH_3CH_2SCH_2$py would be expected. This indeed happens for the bridging methylene between the sulfur and the pyridine moieties (3.8 ppm in IIa; 4.3 ppm in Zn(IIa)Br_2), but it does not for the other group (2.5 ppm in IIa; 2.45 ppm in Zn(IIa)Br_2). Since the observed spectroscopic properties were not sufficient to clearly determine the chelating capacity of ligand IIa, an X-ray crystal structure analysis of Zn(IIa)Br_2 was undertaken.

As can be observed in Figure 1, which also shows the atom-labeling scheme, the coordination polyhedron about the zinc atom can be described as a trigonal bipyramid (TBP). The bromide ligands are cis and occupy two of the equatorial positions. The remaining sites are occupied by the sulfur atoms and the nitrogen of the tridentate chelating ligand (IIa). The angle between the normal of the mean planes defined by N-Zn-Br1-Br2 and Zn-S1-S2-N is 85.5°. The C6a and C6b atoms depart from the last mean plane 1.02 Å. In addition, these two planes depart from the pyridine plane -0.03 and +0.05 Å, respectively. Table I contains the final positional parameters. Table II contains the bond lengths and angles. It is interesting to comment on the slightly long S-Zn distances (average 2.7 Å), that could explain the small chemical shift ^{1}H NMR variation of the CH_3CH_2S protons from noncoordinated to coordinated IIa.

Compounds IIb and IIc react readily at room temperature with salts of transition metals in a +2 formal oxidation state, yielding compounds with stoichiometries M(IIb)X_2 (M = Cd, Cu; X = NO_3, Cl) or M(IIc)X_2 (M = Ni, Cd; X = Cl, NO_3). These complexes present, with respect to those of IIa, an enhanced solubility and, as their precursors do, a great tendency for oiling. This has precluded the growth of crystals suitable for X-ray analysis; however, some structural information can be obtained from the spectroscopic data.

The IR spectra of M(IIc)X_2 compounds display N-H absorption bands at 3160 and 3260 cm^{-1}, 100 and 80 cm^{-1} lower than the corresponding ones in IIc, clearly evidencing a M-N bond. Less evidence exists on the pyridine and/or sulfur coordination to the metal, since there are not any bands in the IR spectrum that unambiguously confirm it.

Acknowledgment. This work was supported in part through CAICYT (Ministerio de Educación y Ciencia, Spain) Grant 409-01/84.

Registry No. IIa, 103884-50-0; IIb, 103884-51-1; IIc, 103884-52-2; Ni(IIa)Cl_2, 103884-35-1; Co(IIa)Cl_2, 103884-36-2; Co(IIa)$(NO_3)_2$, 103884-37-3; Ni(IA)Br_2, 103884-38-4; Zn(IIa)Br_2, 103884-39-5; Co(IIa)$(SCN)_2$, 103884-40-8; Ni(IIa)$(SCN)_2$, 103884-41-9; Cu(IIb)Cl_2, 103884-43-1; Cd(IIb)Cl_2, 103884-44-2; Ni(IIb)Cl_2, 103884-45-3; Ni(IIb)$(NO_3)_2$, 103884-46-4; Co(IIb)Cl_2, 103980-73-0; Ni(IIc)Br_2, 103884-42-0; Cd(IIc)$(NO_3)_2$, 103884-47-5; Cu(IIc)Cl_2, 103884-48-6; Co(IIc)Cl_2, 103884-49-7; 2,6-bis(bromomethyl)pyridine, 7703-74-4; ethanethiol, 75-08-1; 2-mercaptoethanol, 60-24-2; cysteamine hydrochloride, 156-57-0.

Supplementary Material Available: Tables of positional parameters, bond distances to hydrogen atoms, and anisotropic thermal parameters (U's) (3 pages); a table of observed and calculated structure factors (13 pages). Ordering information is given on any current masthead page.

Contribution from the Department of Chemistry, Virginia Polytechnic Institute and State University, Blacksburg, Virginia 24061

Variable-Temperature Magic-Angle-Spinning ^{13}C NMR of Solid $Fe_3(CO)_{12}$

Brian E. Hanson,* Edward C. Lisic, John T. Petty, and Gennaro A. Iannaconne

Received October 31, 1985

Several years ago we reported that the room-temperature magic-angle-spinning (MAS) ^{13}C NMR spectrum of solid $Fe_3(CO)_{12}$ is consistent with rapid bridge-terminal exchange of carbonyls occuring in the solid state.[1] Broad-line NMR results for $Fe_3(CO)_{12}$ were also reported to be consistent with a dynamic process in the solid state.[2] We have now obtained MAS ^{13}C NMR spectra for $Fe_3(CO)_{12}$ at temperatures down to -93 °C. These show, for the first time, a spectrum consistent with the static structure of $Fe_3(CO)_{12}$.

Experimental Section

Triiron dodecacarbonyl (Pressure Chemicals) was enriched in ^{13}CO by stirring a methylene chloride solution of $Fe_3(CO)_{12}$ under an atmosphere of enriched carbon monoxide in the presence of 10 mg of 5% Pd/C. The level of enrichment was determined by mass spectroscopy to be 18%. The enriched $Fe_3(CO)_{12}$ was recrystallized from pentane prior to use.

(1) Dorn, H. C.; Hanson, B. E.; Motell, E. *Inorg. Chim. Acta* **1981**, *74*, L71.
(2) Gleeson, J. W.; Vaughan, R. W. *J. Chem. Phys.* **1983**, *78*, 5384.

0020-1669/86/1325-4062$01.50/0

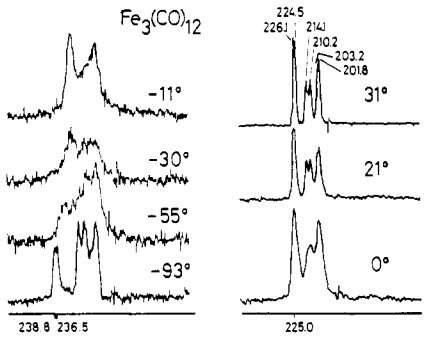

Figure 1. Variable-temperature MAS ^{13}C NMR for solid $Fe_3(CO)_{12}$. At −93 °C bridging carbonyls are observed at 238.8 and 236.5 ppm. In the terminal region three broad resonances at 216.0, 209.5, and 198.3 ppm are observed. The integration of bridging to terminal carbonyls is 2:10, and within the terminal region the approximate relative intensities are 2:4:4. This indicates some accidential degeneracy of signals in the terminal region.

All magic-angle-spinning NMR spectra were recorded at 22.6 MHz by using the following instrumentation: a Chemagnetics superconducting magnetic at a field of 2.12 T, a Chemagnetics variable-temperature ^{13}C probe tuned to 22.6 MHz, and a Chemagnetics variable-temperature controller. The magnet is interfaced to a JEOL FX60Q console. All RF conversions were made locally at VPI & SU.

Estimates of the ^{13}C T_1 for $Fe_3(CO)_{12}$ were made by the progressive-saturation technique.[3] The spectra at 21 and 31 °C consist of 30 $\pi/2$ pulses with a pulse delay of 4 min. At −11 and −30 °C five $\pi/2$ pulses were recorded also with a pulse delay of 4 min. The spectra at −55 °C and below were recorded with a single $\pi/2$ pulse on a sample that had been cooled directly to the desired temperature without experiencing an RF pulse. The temperatures reported are those given by the thermocouple of the Chemagnetics temperature controller. This thermocouple is placed in the spinner air steam immediately before the sample. Prior to recording of the NMR spectrum the sample was equilibrated for 10 min at the reported temperatures; furthermore, the temperature did not fluctuate more than ±2 °C at any temperature setting.

Results and Discussion

The dominant spin–lattice relaxation mechanism for metal carbonyls appears to be chemical shift anisotropy (CSA).[2,4] Consistent with this, solid $Fe_3(CO)_{12}$ shows a small field dependence in T_1: T_1 = 80 s at 15 MHz and ca. 50 s at 22.6 MHz at 25 °C. It should be emphasized that these values are estimates obtained by the progressive-saturation technique and are not very precise. The values however are consistent with a major contribution of the CSA mechanism to the overall T_1 value.

The T_1 value for solid $Fe_3(CO)_{12}$ is strongly dependent on temperature. In one experiment at −121 °C T_1 was estimated to be greater than 1 h by progressive saturation. In view of the exceptionally long T_1 value at low temperature all spectra below −55 °C were recorded on a sample that had been cooled directly to the appropriate temperature without experiencing an RF pulse. The long T_1 value observed at low temperature is consistent with very slow molecular motions.

Variable-temperature MAS ^{13}C NMR spectra for solid $Fe_3(CO)_{12}$ are shown in Figure 1 from 31 to −93 °C. The spectrum at 31 °C agrees well with the spectrum previously reported at 25 °C for $Fe_3(CO)_{12}$ at 15 MHz. At a comparable temperature (21 °C) in the present study the line widths are much broader than obtained previously. This is due to the field dependence of the line shape for a dynamic molecule;[3] i.e., at the higher field higher temperatures are required to obtain coalescence of signals.

The most important feature apparent in these spectra is the fate of the two resonances at 224.5 and 226.1 ppm as the temperature is lowered. All peaks broaden as the temperature is lowered to −55 °C, and finally at −93 °C they begin to sharpen again as motions become slow on the NMR time scale. (At −121 °C no further resolution of the signal is observed.) The peaks at 224.5 and 226.1 ppm are no longer present at −93 °C; however, new peaks at 238.8 and 236.5 ppm appear in this spectrum. These represent bridging carbonyls and agree well with the value observed for solid $Fe_2(CO)_9$.[5] (The resolution at −93 °C is not sufficient to assign two discrete signals in the bridging region. However, collectively the 238.8 and 236.5 ppm signals integrate for two carbonyls. The integration combined with the chemical shift allows the assignment of these peaks to bridging carbonyls.) The integrated intensity of the bridging carbonyl peaks to all of the terminal carbonyl peaks (i.e. those from 198 to 216 ppm) is 2:10, consistent with the molecular structure for $Fe_3(CO)_{12}$ as determined by X-ray crystallography.[6] It is clear from Figure 1 that $Fe_3(CO)_{12}$ is fluxional in the solid state on the NMR time scale and that the dynamic process exchanges bridging and terminal carbonyls.

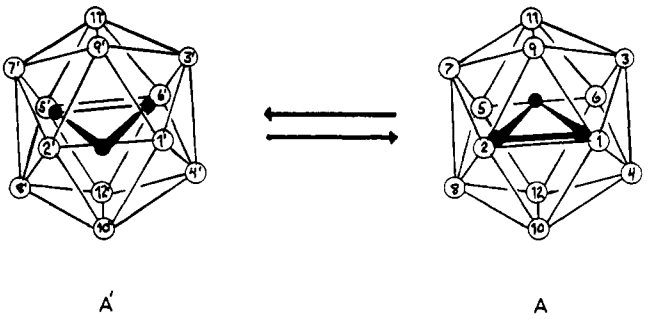

Figure 2. Idealized representation of the structure of $Fe_3(CO)_{12}$. The numbering scheme is the same as previously reported.[1] Vertices 9 and 10 represent bridging carbonyls in A; 9′ and 10′ are in terminal positions in A′. The crystal structure shows the space average of these two orientations. The room-temperature NMR spectrum is consistent with the time average of both orientations. Thus, the motion involves rotation of the iron triangle within the polyhedron of carbonyls.

The line widths in the low-temperature spectra are very much broader than those observed in the fast-exchange limit. This may be due to ^{13}C–^{13}C dipolar interactions in the slow-exchange limit.

As discussed previously,[1] the mechanism that best accounts for bridge–terminal exchange as well as exchanging terminal carbonyls in pairs of two to give the six-line spectrum observed at high temperature involves rotation of the iron triangle within the polyhedron defined by the carbonyl ligands. For clarity this is shown again in Figure 2. It has been noted that the 12 carbonyls of $Fe_3(CO)_{12}$ define a distorted icosahedron in the solid state.[6a] Thus, in Figure 2 triiron dodecacarbonyl is represented as an idealized icosahedron.

$Fe_3(CO)_{12}$ crystallizes in the space group $P2_1/n$ with two molecules per unit cell. The cluster occupies a site with inversion symmetry and therefore is disordered in the solid state. The X-ray crystal structure shows the space average of two orientations related by the inversion center; these are designated A and A′ in Figure 2. Rotation of the iron triangle by 60° interchanges A and A′ and interchanges the chemical shifts of 6 pairs of CO's: 1,5; 2,6; 3,4; 7,8; 9,12; and 10,11. These are the positions that are related by the crystallographic inversion center. The high-temperature NMR spectrum therefore has six carbonyl peaks, as required for the time average of the two orientations. The peaks at 226.1 and 224.5 ppm at 31 °C are assigned to carbonyls 9, 10, 11, and 12. At −93 °C the two orientations are equivalent in the NMR yet are not exchanging rapidly. Thus, the peaks at 238.8 and 236.5 ppm are assigned to carbonyls 9 and 10 (Figure 2A). An activation energy of 10 kcal mol^{-1} is estimated from the approximate coalescence temperature of −55 °C for bridge–terminal exchange.[7]

(3) Becker, E. D. *High Resolution NMR. Theory and Chemical Applications*; Wiley-Interscience: New York, 1978.
(4) Hanson, B. E. In *Advanced in Dynamic Stereochemistry*; Gielen, M., Ed.; Freund: London, 1985.
(5) Dorn, H. C.; Hanson, B. E.; Motell, E. *J. Organomet. Chem.* **1982**, *224*, 181.
(6) (a) Wei, C. H.; Dahl, L. F. *J. Am. Chem. Soc.* **1969**, *91*, 1351. (b) Cotton, F. A.; Troup, J. M. *J. Am. Chem. Soc.* **1974**, *96*, 4155.
(7) The slow-exchange limiting spectrum obtained at −93 °C is not of sufficient quality to allow a line shape analysis.

Rotation of the iron triangle in $Fe_3(CO)_{12}$ confirms, in part, the ideas originally proposed by Johnson[8] to explain the fluxional behavior of this molecule.

Acknowledgment. We thank the NSF for support of this work (Grant DMR-8211111). We thank Professor Harry C. Dorn for his assistance in constructing the NMR equipment.

Registry No. $Fe_3(CO)_{12}$, 17685-52-8.

(8) Johnson, B. R. G. *J. Chem. Soc., Chem. Commun.* **1976**, 703.

Contribution from the Department of Chemistry, Indian Institute of Technology, Kanpur 208 016, India

Linkage Isomers of the Pentaammine(selenocyanato)ruthenium(III) Cation: Synthesis and Characterization

V. Palaniappan and U. C. Agarwala*

Received January 27, 1986

In continuation of our earlier investigations on the linkage isomerism of the thiocyanate ligand,[1-5] the possibility of selenocyanate ion exhibiting linkage isomerism in similar systems was speculated. The simple and classical substitution reactions of $[(NH_3)_5RuX]X_2$ (X = Cl, Br, I) with thiocyanate ion simultaneously generate two linkage isomers, viz., $[(NH_3)_5RuNCS]^{2+}$ and $[(NH_3)_5RuSCN]^{2+}$ ions, with the yield of S-isomer approximately one-third of that of N-isomer.[1b,2b] Furthermore, the literature survey reveals practically no study on the ruthenium complexes having selenocyanate ion as coligand.[6]

During the course of our studies on the linkage isomerism of selenocyanate we encountered some problems in the published procedure for the synthesis.[7] We have, therefore, made a thorough reexamination of the syntheses and purification of the complexes, the results of which are reported herein, with a method to separate the Se- and N-bonded isomers of the selenocyanate ligand.

Experimental Section

Materials. All chemicals used were of chemically pure or of AnalaR grade. Doubly distilled water was used throughout. $[(NH_3)_5RuX]X_2$ (X = Cl, Br) were prepared by the published procedures.[8] Potassium selenocyanate was obtained from Fluke AG and was used without further purification. Sephadex G-10 (40-120 mesh), Sephadex LH-20 (25-100 mesh), Dowex 1-X8 (100-200 mesh) in Cl^- form, and Dowex 50W-X8 (200-400 mesh) in Na^+ form were used for chromatographic studies.

Preparations. (a) $[(NH_3)_5RuSeCN]I_2\cdot 2H_2O$ and $[(NH_3)_5RuNCSe]I_2\cdot 2H_2O$. A typical reaction carried out is as follows. An aqueous solution (8-10 mL) of approximately 10 times the stoichiometric excess of potassium selenocyanate was added to an aqueous solutin (15-20 mL) of $[(NH_3)_5RuX]X_2$ (X = Cl or Br) (0.2 g) maintained at 50-60 °C. The solution was stirred vigorously until the reaction mixture turned bright blue (~10 min; stirring for longer periods deposited selenium powder). The resulting solution was cooled to room temperature and was filtered from the selenium powder into a saturated solution of potassium iodide. The solution, when cooled at 0 °C, yielded a greenish blue precipitate, which was filtered and washed several times with ethanol and with ether.

The greenish blue compound was dissolved in a minimum quantity of water and was sorbed onto a column of cation exchanger in Na^+ form (20 x 2 cm). It was eluted with potassium iodide solution of different molarities. The elution with 1 and 4 M potassium iodide solution gave minor amounts of monopositive and tetrapositive species, which are being studied presently.[5] The eluate from 2 M potassium iodide solution elution was collected and concentrated at room temperature, which yielded a violet-green compound, after the addition of saturated potassium iodide solution (yield 70-80%). From the IR and electronic spectra, it was found to be a mixture of both N- and Se-bonded isomers. This was further corroborated later, by recording the IR and electronic spectra of the mixture containing authentic samples of both isomers.

The violet-green compound (mixture of Se- and N-isomers) was dissolved in a minimum amount of water and was sorbed into a Sephadex G-10 column (50 × 2 cm). It was eluted with a 10^{-5} M solution of potassium iodide. With a very slow elution rate (3-4 mL/h), clear separation of two bands (band I, pink; band II, blue) was observed. The bands were eluted separately, and the eluates were concentrated at room temperature; a saturated solution of potassium iodide was added separately to the concentrates of pink and blue solutions to precipitate $[(NH_3)_5RuSeCN]I_2\cdot 2H_2O$ and $[(NH_3)_5RuNCSe]I_2\cdot 2H_2O$, respectively (yields 8-12% and 45-50% based on $[(NH_3)_5RuX]X_2$).

(b) $[(NH_3)_5RuSeCN](ClO_4)_2\cdot 2H_2O$ and $[(NH_3)_5RuNCSe](ClO_4)_2\cdot 2H_2O$. The procedure used to prepare these complexes was the same as that described in (a) except that sodium perchlorate was used in place of potassium iodide. Purple $[(NH_3)_5RuSeCN](ClO_4)\cdot 2H_2O$ and Prussian blue colored $[(NH_3)_5RuNCSe](ClO_4)_2\cdot 2H_2O$ were precipitated from the concentrates of first and second band eluates, respectively.

(c) $[(NH_3)_5RuSeCN]Cl_2\cdot 2H_2O$ and $[(NH_3)_5RuNCSe]Cl_2\cdot 2H_2O$. As the direct precipitation of chloride salts was not possible, anion-exhange resin in Cl^- form was used. The iodide salts of the complexes were sorbed into the anion-exchange column (50 × 1 cm), and the compounds were eluted with water. The eluates were evaporated partially at room temperature. The chloride salts, viz., $[(NH_3)_5RuSeCN]Cl_2\cdot 2H_2O$ and $[(NH_3)_5RuNCSe]Cl_2\cdot 2H_2O$, precipitated and were centrifuged and washed with ethanol and ether.

(d) $[(NH_3)_5RuSeCN]Br_2\cdot 2H_2O$ and $[(NH_3)_5RuNCSe]Br_2\cdot 2H_2O$. The procedure for the syntheses of these complexes was the same as described in (c) except that the anion-exchange resin used was in bromide form instead of chloride form. After concentration of the eluates at room temperature, bluish purple $[(NH_3)_5RuSeCN]Br_2\cdot 2H_2O$ and blue $[(NH_3)_5RuNCSe]Br_2\cdot 2H_2O$ were precipitated.

(e) $[(NH_3)_5RuNCSe](BPh_4)_2$ and $[(NH_3)_5RuSeCN](BPh_4)_2$. A concentrated solution of the bromide or chloride salt of the N- or Se-isomer was added to a solution of $NaBPh_4$ in acetone. The solution was left at 0 °C for several hours, and subsequently the cooled solution was concentrated at reduced pressure, whereupon green or dark green water-insoluble $[(NH_3)_5RuNCSe](BPh_4)_2$ or $[(NH_3)_5RuSeCN](BPh_4)_2$ precipitated. The product was centrifuged and washed with a little ethanol and ether. Both isomers are soluble in ethanol and acetone.

(f) $[(NH_3)_5RuNCSe](C_7H_7SO_3)_2$ and $[(NH_3)_5RuSeCN](C_7H_7SO_3)_2$. The procedure used to synthesize the complexes was the same as that given in (e) except that a saturated solution of sodium *p*-toluenesulfonate in ethanol was used instead of sodium tetraphenylborate in acetone. The precipitated greenish blue compound $[(NH_3)_5RuNCSe](C_7H_7SO_3)_2$ or green $[(NH_3)_5RuSeCN](C_7H_7SO_3)_2$ was centrifuged and washed with ethanol and ether.

All the experiments were carried out under acid-free atmosphere, as even traces of acid decomposed selenocyanate, depositing selenium powder.

In all of the above procedures, the compounds, either as solids or in solution, were preserved at 0 °C, as at room temperature they have a tendency to decompose to an insoluble polymeric form along with the deposition of some selenium powder. The purity of the compounds was checked at intervals by passing the solutions through Sephadex G-10. In the case of the BPh_4^- salt, Sephadex LH-20 was used instead of Sephadex G-10.

Physical Measurements. Analyses for carbon, hydrogen, and nitrogen were done by the Microanalytical Section, Indian Institute of Technology, Kanpur. Selenium was estimated by oxidizing to selenate, followed by reducing it to selenite by boiling with concentrated HCl and finally to selenium powder by hydroxylammonium chloride.[9,10] Analyses for sulfur and halogen were carried out by known procedures. IR spectra were

(1) (a) Parashad, R.; Yadav, S. K. S.; Agarwala, U. C. *J. Inorg. Nucl. Chem.* **1981**, *43*, 2359. (b) Parashad, R. Ph.D. Thesis, IIT, Kanpur, India, 1980.
(2) (a) Yadav, S. K. S.; Agarwala, U. C. *Polyhedron* **1984**, *3*, 1. (b) Yadav, S. K. S. Ph.D. Thesis IIT, Kanpur, India, 1982.
(3) Yadav, S. K. S.; Agarwala, U. C. *Indian J. Chem. Sect. A* **1982**, *21A*, 175.
(4) Palaniappan, V.; Yadav, S. K. S.; Agarwala, U. C. *Polyhedron* **1985**, *4*, 1457.
(5) Palaniappan, V.; Agarwala, U. C., results to be submitted for publication.
(6) Norbury, A. H. *Adv. Inorg. Chem. Radiochem.* **1975**, *17*, 231.
(7) Lin, S. W.; Schreiner, A. F. *Inorg. Chim. Acta* **1971**, *5*, 290.
(8) Allen, A. D.; Bottomley, F.; Remsolu, V. P.; Senoff, C. V. *J. Am. Chem. Soc.* **1967**, *89*, 5595.
(9) Vogel, A. I. *A Textbook of Quantitative Inorganic Analysis*, 2nd ed.; Longmans, Green and Co.: London, 1951; p 441.
(10) Williams, J. W. *Handbook of Anion Determination*; Butterworths: London, 1979.

0020-1669/86/1325-4064$01.50/0